JOURNAL OF APPLIED ELECTROCHEMISTRY 9 (1979) 427–435

Dispersion in electrochemical cells with radial flow between parallel electrodes. I. A dispersive plug flow mathematical model

M. FLEISCHMANN, R. E. W. JANSSON

Chemistry Department, The University, Southampton, UK

Received 21 November 1977

The conventional relations for dispersion in tubes and ducts are inappropriate for radial flows such as are found in the disc-stack and pump cells. A first-order mathematical model is therefore developed for radial flow between infinite parallel planes. The shapes of the predicted responses to pulses of injected material are shown to be in qualitative agreement with experimental curves, however the form of the mathematical expression is inappropriate for routine data analysis. Nevertheless simple relationships are derived which enable the dispersion coefficient and mean residence time of an electrogenerated species to be determined from the first and second moments of the response and a knowledge of the geometry of the system. In Part II experimental data are analysed in detail with the aid of the model; however, it is clear that an improved model is of a three-phase flow, a slow phase creeping along either plane with a faster 'core' flow in between.

List of Symbols

c concentration (mol cm^{-3})
$\bar{D}$ dispersion coefficient (cm^2 s^{-1})
h interelectrode gap (cm)
M_1 normalized first moment of the response defined by Equation 28
M_2 normalized second moment of the response, defined by Equation 29
$Q = V/h$ volumetric flow rate per unit height of gap (cm^2 s^{-1})
$q = (s/\bar{D})^{1/2}$ (cm)
r radius (cm)
s Laplace transform parameter (s^{-1})
t time (s)
V volumetric flow rate per unit height
$x = (r - r_i)/2(\bar{D}t)^{1/2}$ dimensionless distance
$\nu = Q/(4\pi\bar{D})$
$\lambda = r(s/\bar{D})^{1/2}$
$\tau = M_1$ mean residence time of marked material(s)

Subscripts

i inner
o outer

1. Introduction

A number of cells with radial outflow (source flow) of electrolyte between parallel planes are in industrial use or under laboratory investigation; these include the well-known capillary gap cell of Beck and Guthke [1], now often called the disc-stack cell, the electrochemical pump cell [2, 3] and the rotating electrolyser [4]. Whether or not the electrodes have rotational motion, all these cells have in common the deceleration of the radial component of flow due to the increase in channel cross-sectional area with radius, which can have an important effect upon the specificity of some synthetic reactions [5, 6]. Further, the specificity where competing reactions occur is strongly a function of local conditions, such as species concentration and pH, and is therefore tied to the prevailing transport conditions [6]. In fact the chemical and transport rates are coupled, as in combustion.

Under creeping flow conditions in a capillary gap cell [7] the only transport process in operation is molecular diffusion, which is slow and leads to high concentrations of electro-

0021–891X/79/040427–09 $02·90/0

generated species close to an electrode surface, favouring reactions of high order. Where competing reactions can occur it would be surprising if the same distribution of products was obtained at high and low flow rates, since the mixing regimes are different in these two cases. Likewise, in the pump cell, where the predominant transport mechanism is turbulent dispersion induced by the tangential shear, a different distribution of products is obtained from that for a geometrically identical capillary gap cell operating at the same volumetric flow rate [6].

Generally it has not been recognised explicitly that the outcome of a particular synthetic reaction in a particular cell may depend upon the coupling of chemical and transport rates, so that a reaction which fails in one kind of cell may succeed in another, simply due to one cell having a more favourable reaction environment. A prerequisite for further advance in this respect is information on the magnitudes of dispersion and mixing processes in technical cells. Using an electrochemical analogue [9] of the marker pulse technique of chemical engineering [11] it is possible to obtain a measure of dispersion in electrochemical systems with comparative ease [8, 9, 12]. The results, however, are only quantitatively analysable with the aid of an appropriate mathematical model for the reactor.

The mathematical modelling of dispersion in reacting radial source flow is extremely difficult, requiring effectively the simultaneous solution of the full Navier–Stokes and time-dependent transport and chemical rate equations. As a first step in tackling this problem it was decided to adopt the simplest possible mathematical model which would represent the time-history of a marker pulse so that the reaction environment in cells with radial flow could at least be classified. It was also expected that, as in the case of conventional reaction engineering, trends in experimental data analysed with the aid of the simplest model would suggest improvements which could be made to give an adequate description of the reaction environment without the need to solve the full, coupled problem.

The development of the mathematical model is discussed in Part I of this paper; experimental data analysed with its aid are discussed in detail in Part II.

2. Model

Consider the radial outflow of electrolyte between infinite parallel planes (Fig. 1). Normally there is a velocity distribution in the axial direction, z, due to viscous drag at the bounding planes, but the model adopted in this exploratory work is of dispersive radial plug flow, i.e. all fluid elements at the same radius are assumed to move with the same average speed regardless of their distances from the bounding planes (electrodes), and the effects of the real velocity gradient are lumped together with the effects of fluctuations into a term representing dispersion in the radial direction. (The latter will be called 'radial dispersion' since, in this co-ordinate system, the axial direction is not the direction of mean mass flow.) If the volumetric flow rate per unit height of inter-electrode gap is Q, then, at any distance $r > r_e$, the equation of continuity gives

$$u(r) = Q/2\pi r \tag{1}$$

and a mass balance on any annular control volume $2\pi r dr \Delta z$ for any species of local concentration $c(r)$ at $r = r$, in the absence of reaction, gives,

$$\frac{\partial c}{\partial t} = \bar{D}\frac{\partial^2 c}{\partial r^2} + \frac{\bar{D}}{r}\frac{\partial c}{\partial r} - \frac{Q}{2\pi r}\frac{\partial c}{\partial r} \tag{2}$$

where $\bar{D}$ represents the radial dispersion coefficient, i.e. in the direction of mean flow.

If the concentration of marker species is injected uniformly at $r = r_i$, the initial condition is normally

$$c = 0, \quad 0 < r < \infty \tag{3}$$

so that, on Laplace transforming Equation 2, one obtains

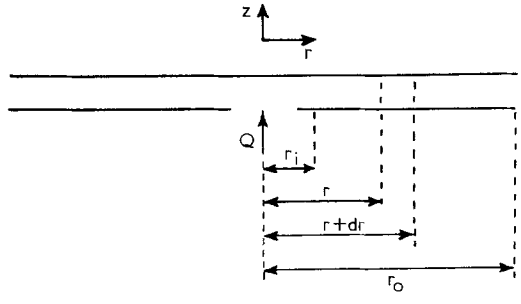

Fig. 1. Co-ordinate system for radial source flow between infinite parallel planes.

$$\frac{d^2\bar{c}}{dr^2}+\left(\frac{1}{r}-\frac{Q}{2\pi r\bar{D}}\right)\frac{d\bar{c}}{dr}-\frac{s}{\bar{D}}\bar{c}=0 \qquad (4)$$

which may be written as

$$\frac{d^2\bar{c}}{dr^2}+\left(\frac{1-2\nu}{r}\right)\frac{d\bar{c}}{dr}-\frac{s}{\bar{D}}\bar{c}=0 \qquad (5)$$

if

$$\nu = Q/4\pi\bar{D}. \qquad (6)$$

To simplify Equation 5 let

$$\lambda = r(s/\bar{D})^{1/2} \qquad (7)$$

when

$$\frac{d^2\bar{c}}{d\lambda^2}+\frac{(1-2\nu)}{\lambda}\frac{d\bar{c}}{d\lambda}-\bar{c}=0 \qquad (8)$$

and assume that Equation 8 has a solution of the form

$$\bar{c} = \lambda^{\gamma}\omega \qquad (9)$$

with a suitable choice for γ. Successive differentiation of Equation 9 and substitution back into Equation 8 gives

$$\frac{d^2\omega}{d\lambda^2}+\frac{(2\gamma-1-2\nu)}{\lambda}\frac{d\omega}{d\lambda}-\left[1-\frac{\gamma(\gamma-1)+\gamma(1-2\nu)}{\lambda^2}\right]\omega=0 \qquad (10)$$

Now, choosing γ such that

$$2\gamma+1-2\nu = 1$$

i.e.

$$\gamma = \nu$$

Equation 10 becomes

$$\frac{d^2\omega}{d\lambda^2}+\frac{1}{\lambda}\frac{d\omega}{d\lambda}-\left(1+\frac{\nu^2}{\lambda^2}\right)\omega=0 \qquad (11)$$

which is a *modified Bessels equation*, the solutions to which [10, 14] are $I_\nu(\lambda)$, $I_{-\nu}(\lambda)$ and $K_\nu(\lambda)$ with *no* restrictions on ν, all of which are real when ν is real and λ is positive. Now $I_{\pm\nu}(\lambda)\to\infty$ as $\lambda\to\infty$ while $K_\nu(\lambda)\to 0$ as $\lambda\to\infty$ and the physics of the situation demands that

$$\bar{c}\to 0 \text{ as } \lambda\to\infty, \quad \text{i.e. } r\to\infty$$

since the concentration of injected marker must ultimately fall to zero at large enough radius. The appropriate solution to Equation 11 is therefore given by $K_\nu(\lambda)$.

When ν is not an integer or zero,

$$K_\nu(\lambda) = \tfrac{1}{2}\pi(\sin\nu\pi)^{-1}[I_{-\nu}(\lambda)-I_\nu(\lambda)]$$

and (12)

$$I_\nu(\lambda) = \sum_{n=0}^{\infty}(\lambda/2)^{\nu+2n}\Big/ n!\Gamma(\nu+n+1)$$

but, when $\nu = n$ is an integer

$$I_{-n}(\lambda) = I_n(\lambda) \qquad (13)$$

and Equation 12 is indeterminate, so it is necessary [10] to take

$$K_\nu(\lambda) = \lim_{\nu\to n}K_\nu(\lambda) = (-1)^n\frac{1}{2}\left(\frac{\partial I_{-\nu}}{\partial\nu}-\frac{\partial I_\nu}{\partial\nu}\right)_{\nu=n} \qquad (14)$$

from which the value for $\nu = n = 0$ can also be obtained [10]. With the definitions of Equations 12 and 14 K_ν is an entire function of ν and the solution of Equation 8 is, therefore

$$\bar{c} = A\lambda^{\nu}K_\nu(\lambda) \qquad (15)$$

with *no* restrictions on ν.

If a step in concentration is made at $r = r_i$, i.e.

$$c = c_o \text{ or } \bar{c} = \frac{c_o}{s} \text{ at } r = r_i$$

then from Equation 15

$$\bar{c} = \frac{c_o}{s}\left(\frac{r}{r_i}\right)^{\nu}\frac{K_\nu[r(s/\bar{D})^{1/2}]}{K_\nu[r_i(s/\bar{D})^{1/2}]} \qquad (16)$$

with $\nu = Q/4\pi\bar{D}$, since $\lambda = r(s/\bar{D})^{1/2}$, and for a delta function in concentration

$$\bar{c} = c_o\left(\frac{r}{r_i}\right)^{\nu}\frac{K_\nu[r(s/\bar{D})^{1/2}]}{K_\nu[r_i(s/\bar{D})^{1/2}]}. \qquad (17)$$

In general the Laplace inversion of Equation 17 is difficult; note, for example, that, as $\nu = Q/4\pi\bar{D}$, both the order and the argument are unknown and, under typical experimental conditions (see Part II), ν can be large. However it is possible to obtain the inverse for some simple cases, which is useful as a check on the reasonableness of the simple model.

3. Explicit solutions of Equation 17

Consider the function $K_\nu(\lambda) = K_\nu(qr)$, where $q = (s/\bar{D})^{1/2}$. The asymptotic expansion of $K_\nu(z)$ for $|\arg z| < (3/2)\pi$ is [14]

$$K_\nu(qr) = \left(\frac{\pi}{2qr}\right)^{1/2} \exp\left\{-qr\left[1 + \frac{(4\nu^2 - 1^2)}{1!(8qr)} + \frac{(4\nu^2 - 1)(4\nu^2 - 3^2)}{2!(8qr)^2} + \frac{(4\nu^2 - 1^2)(4\nu^2 - 3^2)(4\nu^2 - 5^2)}{3!(8qr)^3} + \ldots\right]\right\}. \quad (18)$$

Clearly this series will truncate for certain half-integer values of ν. Since there is no restriction on ν, assume, for example, that $\nu = 3/2$, when

$$\frac{K_{3/2}(qr)}{K_{3/2}(qr_i)} = \left(\frac{r_i}{r}\right)^{1/2} \exp\left[-q(r - r_i)\left(1 + \frac{1}{qr}\right)\left(1 + \frac{1}{qr_i}\right)^{-1}\right]. \quad (19)$$

For the case of $qr_i > 1$ this can be expanded immediately to give

$$\frac{K_{3/2}(qr)}{K_{3/2}(qr_i)} = \left(\frac{r_i}{r}\right)^{1/2} \exp\left[-q(r - r_i)\left(1 + \frac{1}{qr}\right) \times \left(1 - \frac{1}{qr_i} + \frac{1}{q^2 r_i^2} - \frac{1}{q^3 r_i^3} + \ldots\right)\right]$$

which can be substituted into Equation 17 to give

$$\bar{c} = c_o\left(\frac{r}{r_i}\right) \exp\left\{-q(r - r_i)\left[1 - \left(\frac{1}{r_i} - \frac{1}{r}\right) \times \left(\frac{1}{q} - \frac{1}{q^2 r_i} + \frac{1}{q^3 r_i^2} - \frac{1}{q^4 r_i^3} + \ldots\right)\right]\right\}$$

which can be inverted term by term to give

$$c = \frac{c_o}{t}\left(\frac{r}{r_i}\right)\left[\frac{x}{\pi^{1/2}} \exp -x^2 - \frac{(r - r_i)^2}{rr_i}\frac{1}{2\pi^{1/2}x} \exp -x^2 + \frac{(r - r_i)^3}{rr_i^2}\frac{1}{4x^2} \operatorname{erfc} x - \frac{(r - r_i)^4}{rr_i^3}\frac{1}{4x^3} i \operatorname{erfc} x + \frac{(r - r_i)^5}{rr_i^4}\frac{1}{4x^4} i^2 \operatorname{erfc} x - \ldots\right] \quad (20)$$

where $x = (r - r_i)/2(\bar{D}t)^{1/2}$ and $i^n \operatorname{erfc} x$ is the nth integral of the error function. Equation 20 can be written more conveniently as

$$\left(\frac{c}{c_o}\right)t = \left(\frac{r}{r_i}\right)\left(a_1 \exp -x^2 - \frac{a_2}{x} \exp -x^2 + \frac{a_3}{x^2} \operatorname{erfc} x - \frac{a_4}{x^3} i \operatorname{erfc} x + \frac{a_5}{x^4} i^2 \operatorname{erfc} x - \frac{a_6}{x^5} i^3 \operatorname{erfc} x + \frac{a_7}{x^6} i^4 \operatorname{erfc} x - \ldots\right). \quad (21)$$

Clearly the series will converge most rapidly for large x and for r of the same order as r_i, i.e. short time delays, small values of dispersion and small radial expansions.

If $qr_i < 1$ then, for $\nu = 3/2$, Equation 17 can be put in the form

$$\bar{c} = c_o\left(\frac{r}{r_i}\right)^{3/2} \exp\left[-q(r - r_i)\frac{(qr + 1)}{(qr_i + 1)}\left(\frac{r_i}{r}\right)^{3/2}\right]$$

$$= c_o \exp\{-q(r - r_i)[1 + q(r - r_i) - q^2 r_i(r - r_i) + q^3 r_i(r - r_i) - \ldots]\}.$$

As before, inverting term by term gives

$$\left(\frac{c}{c_o}\right)t = \frac{1}{2\pi^{1/2}} \exp\left\{-x^2\left[H_1(x) + xH_2(x) - \frac{r}{(r - r_i)}x^2 H_3(x) + \frac{r^2}{(r - r_i)^2}x^3 H_4(x) \ldots\right]\right\}$$

or

$$\left(\frac{c}{c_o}\right)t = \frac{1}{2\pi^{1/2}} \exp\{-x^2[a_1 H_1(x) + a_2 H_2(x) - a_3 H_3(x) + a_4 H_4(x) - \ldots]\} \quad (22)$$

where $H_n(x)$ is the nth order Hermite polynomial of argument $x = (r - r_i)/2(\bar{D}t)^{1/2}$. Since, in general, the modulus of $H_n(x)$ increases rapidly with x, Equation 22 will converge most rapidly for small x and $r \gg r_i$, i.e. long time delays, large values of dispersion and large radial expansions. Equations 21 and 22 are therefore complementary.

For values of ν greater than 3/2 equations of the same form as Equations 21 and 22 are obtained but the simple structures for the coefficients a_n are lost, although the same limiting conditions apply.

4. Numerical calculation of generalized response curves

Fig. 2a shows a plot of $(c/c_o)t$ versus $x = (r - r_i)/(\bar{D}t)^{1/2}$ for $(r/r_i) = 4$, $r_i = 1$ cm, and

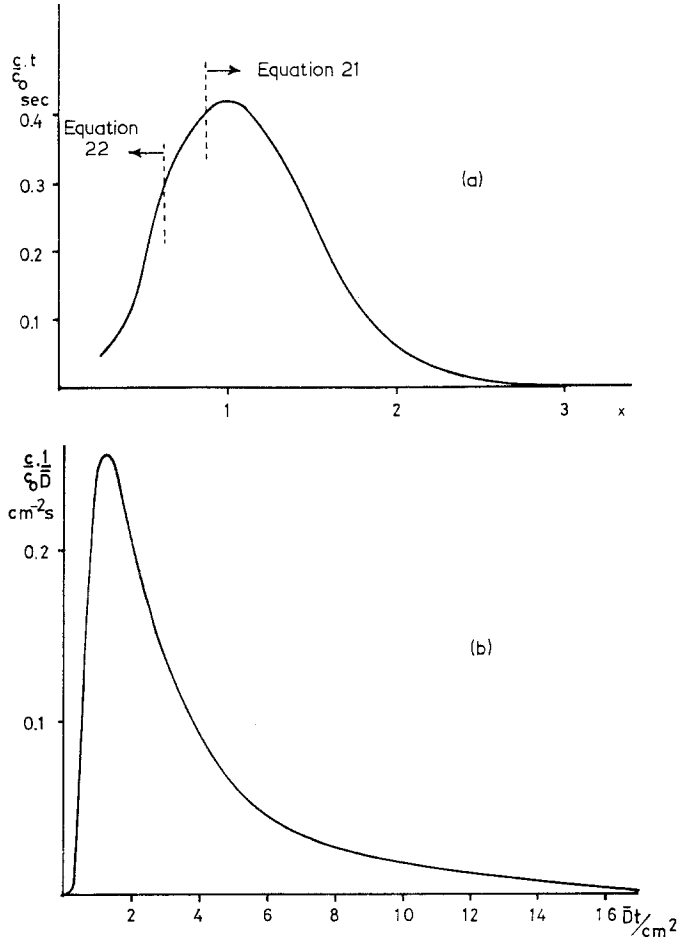

Fig. 2. (a) Numerical simulation of $(c/c_o)t$ versus x using Equations 21 and 22. (b) Transformation of (a) into a generalized response curve.

$\nu = 3/2$, calculated using Equations 21 and 22 for various assumed values of x. There is only a small region, $0{\cdot}6 < x < 0{\cdot}9$, for which neither series converges adequately within 20 terms at this radius ratio. As (r/r_i) decreases the range of applicability of Equation 22 increases, while, conversely, as (r/r_i) increases Equation 21 is applicable over a wider range.

From the definition of x it is clear that

$$\frac{4x^2}{(r-r_i)^2}\left(\frac{c}{c_o}\right)t = \frac{c}{c_o}\frac{1}{\bar{D}} \qquad (23)$$

and

$$\frac{(r-r_i)^2}{4x^2} = \bar{D}t \qquad (24)$$

so the data in Fig. 2a can be transformed into a plot of $(c/c_o)(1/\bar{D})$ versus $\bar{D}t$, as shown in Fig. 2b; this is a generalized response curve to a delta-function pulse at $t = 0$, $r_i = 1$ cm, for $\nu = 3/2 = Q/4\pi\bar{D}$, i.e. $Q = 6\pi\bar{D}$ cm^3 s^{-1} cm^{-1}. In constructing this curve two points have been interpolated from Fig. 2a in the range $0{\cdot}6 < x < 0{\cdot}9$, i.e. the region where no solution to the general equation could be found.

In form, Fig. 2b shows a sharp rise after a short delay, followed by a long tail, and is markedly different to the skew-Gaussian shape of dispersive plug flow in a parallel channel [13]; in particular it should be noted that even this simple model predicts that some species have a residence time in the cell an order longer than the mean time.

The influence of increasing $\nu = Q/4\pi\bar{D}$ on the response curves was investigated by calculating the analagous equation to Equation 21 for $\nu = 1/2$, $3/2$, $5/2$ and $7/2$, assuming $(r/r_i) = 20$ and $r_i = 1$ cm to ensure convergence for $0{\cdot}25 < x < 3$, which covered the range of interest. Even so, up to 30 terms had to be retained in some cases. Fig. 3 shows the normalized generalized response curves. For the sake of clarity the unnormalized curves

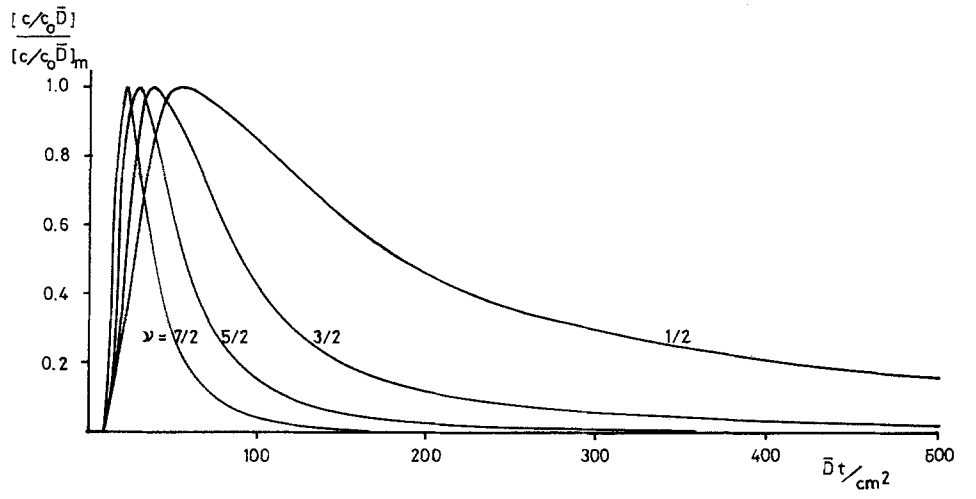

Fig. 3. Synthesized response curves for various values of $\nu = Q/4\pi\bar{D}$.

are not shown, but as ν decreases (increasing $\bar{D}$ at constant Q or increasing Q at constant $\bar{D}$) the calculated curves broaden and decrease in height, which ultimately sets the limit of detectability in the experiments (see Part II). It is also clear, however, that the skewness of the curves depends on ν, with a profound effect on the residence times of the species in the tail.

Detailed discussion of experimental results will be presented in Part II, however the reasonableness of the theory can be seen quantitatively by comparing Fig. 3 with Fig. 4, the results of evoked

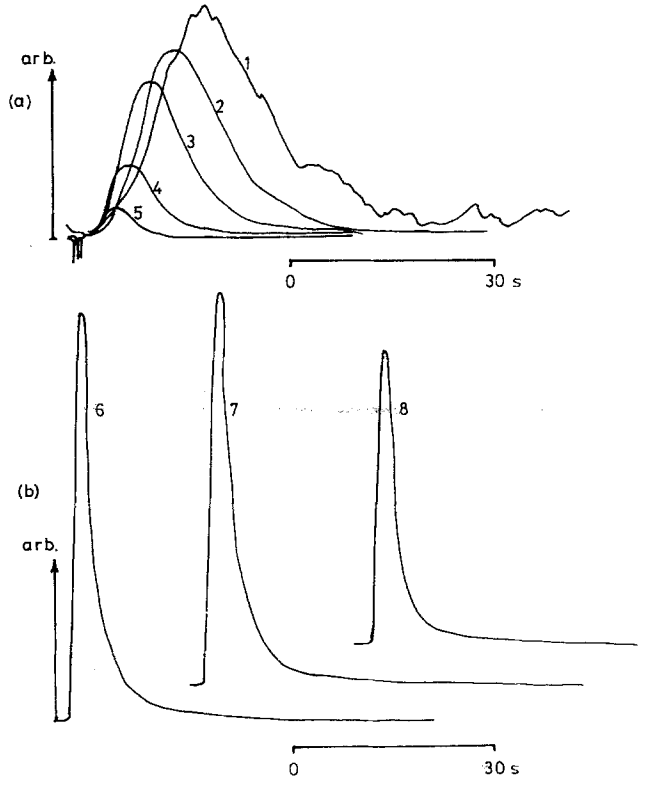

Fig. 4. Experimental response curves for geometrically identical (a) capillary gap cell and (b) pump cell under similar conditions [8]. Curve 1, $(Re) = 0{\cdot}926 \times 10^4$, $(Re)_\phi = 0$; curve 2, $(Re) = 1{\cdot}389 \times 10^4$, $(Re)_\phi = 0$; curve 3, $(Re) = 1{\cdot}852 \times 10^4$, $(Re)_\phi = 0$; curve 4, $(Re) = 2{\cdot}808 \times 10^4$, $(Re)_\phi = 0$; curve 5, $(Re) = 3{\cdot}704 \times 10^4$, $(Re)_\phi = 0$; curve 6, $(Re) = 0{\cdot}926 \times 10^4$, $(Re)_\phi = 6{\cdot}209 \times 10^4$; curve 7, $(Re) = 1{\cdot}852 \times 10^4$, $(Re)_\phi = 6{\cdot}209 \times 10^4$; curve 8, $(Re) = 3{\cdot}704 \times 10^4$, $(Re)_\phi = 6{\cdot}209 \times 10^4$.

response experiments [8] in geometrically identical capillary gap (Fig. 4a) and pump cell (Fig. 4b). Clearly the theoretical and experimental curves have the same general shapes, especially in the case of the pump cell where the mixing due to the tangential shear produces a more uniform axial velocity profile.

5. Numerical analysis of data

In principle it is possible to invert Equation 17 for all values of ν using the definitions in Equations 12 and 14 for K_ν and to find the best fit of the experimental data to a library of computed functions, thus finding ν, hence $\bar{D}$. However this process would be very inefficient and probably not unambiguous, given the errors due to truncation of the function and noise in the response signal. Further, $\bar{D}$ can only be obtained from ν if Q is unambiguous, i.e. the flow is truly plug-like, which is not so (see Section 6). An alternative strategy is to proceed via moment analysis.

6. Moment analysis

The moments of the response are given by

$$m_0 = \underset{s\to 0}{\overset{-1}{\mathscr{L}}}\,(\bar{c}/s) \tag{25}$$

where $\bar{c}$is now the response to a delta-function, i.e. defined by Equation 17

$$m_1 = -(\mathrm{d}\bar{c}/\mathrm{d}s)_{s\to 0} = \int_0^\infty tc\,\mathrm{d}t \tag{26}$$

and

$$m_2 = (\mathrm{d}^2\bar{c}/\mathrm{d}s^2)_{s\to 0} = \int_0^\infty t^2 c\,\mathrm{d}t. \tag{27}$$

The normalized moments are therefore

$$M_1 = m_1/m_0 \tag{28}$$

and

$$M_2 = m_2/m_0. \tag{29}$$

Thus what is needed is the first and second differential of $K_\nu(\lambda)$ as $\lambda \to 0$. Since in general ν is large, $K_\nu(\lambda)$ approximates to $I_{-\nu}(\lambda)$ under these conditions (see Equation 12):

$$\begin{aligned} K_\nu(\lambda) &\cong \frac{\pi}{2\sin\nu\pi} I_{-\nu}(\lambda) \\ &= \frac{\pi}{2\sin\nu\pi(\lambda/2)^\nu} \sum_{n=0}^{\infty} \frac{(\lambda/2)^{2n}}{n!\Gamma(-\nu+n+1)} \end{aligned} \tag{30}$$

Writing $r(s/\bar{D})^{1/2} = qr$ one obtains

$$\begin{aligned} \bar{c} \cong\ & c_0\left(\frac{r}{r_i}\right)^\nu\left(\frac{r_i}{r}\right)^\nu \\ & \times \frac{\left[\dfrac{1}{\Gamma(1-\nu)} + \dfrac{(qr/2)^2}{\Gamma(2-\nu)} + \dfrac{(qr/2)^4}{2\Gamma(3-\nu)} + \ldots\right]}{\left[\dfrac{1}{\Gamma(1-\nu)} + \dfrac{(qr_i/2)^2}{\Gamma(2-\nu)} + \dfrac{(qr_i/2)^4}{2\Gamma(3-\nu)} + \ldots\right]} \end{aligned}$$

or

$$\begin{aligned} \bar{c} \cong\ & c_0\left\{1 + \frac{(r^2-r_i^2)}{4(1-\nu)}\,\frac{s}{\bar{D}}\right. \\ & + \frac{[(1-\nu)r^4 - (4-2\nu)r^2r_i^2 + (3-\nu)r_i^4]}{32(2-\nu)(1-\nu)^2} \\ & \left. \times \left(\frac{s}{\bar{D}}\right)^2 + \ldots\right\} \end{aligned} \tag{31}$$

where use has been made of the recurrence relations of gamma-functions [14]. From Equation 31 it is clear that

$$m_0 = c_0 \tag{32}$$

$$M_1 = -\frac{1}{m_0}\left(\frac{\mathrm{d}\bar{c}}{\mathrm{d}s}\right)_{s\to 0} = -\frac{(r^2-r_i^2)}{4(1-\nu)\bar{D}} \tag{33}$$

and

$$\begin{aligned} M_2 &= \frac{1}{m_0}\left(\frac{\mathrm{d}^2\bar{c}}{\mathrm{d}s^2}\right)_{s\to 0} \\ &= \frac{[(1-\nu)r^4 - (4-2\nu)r^2r_i^2 + (3-\nu)r_i^4]}{16(2-\nu)(1-\nu)^2\bar{D}^2} \end{aligned} \tag{34}$$

Using the definition of ν, Equation 33 becomes

$$M_1 = -\frac{(r^2-r_i^2)}{4(1-Q/4\pi\bar{D})\bar{D}}$$

and if $Q \gg 4\pi\bar{D}$

$$M_1 \cong \pi(r^2-r_i^2)/Q = \tau \tag{35}$$

i.e., if the plug flow model is valid the first moment of the response should approximate to the volumetric residence time for plug flow. It will be shown in Part II that the residence time of the marked fluid close to the electrode in a practical electrolyser may be as much as two orders of

magnitude greater than the mean volumetric residence time, so that even if the marked material proceeds in a plug flow it cannot be the same plug flow as the majority of the electrolyte, i.e. a better model is of two plug flows, one fast one slow. The difficulty now is that Q for the slow, marked flow is undetermined, however it can be eliminated by combining the first and second moments to give an expression for $\bar{D}$ without *explicit* dependence on Q:

$$\bar{D} = \frac{(r^2 - r_i^2)}{4M_1\left\{1 + \frac{(r^2 + r_i^2)}{(r^2 - r_i^2)}\frac{M_1^2}{(M_2 - M_1^2)}\right\}} \quad (36)$$

Equation 36 allows an evaluation of experimental data *as if it were* due to a plug flow (of unknown thickness) proceeding down the wall, and Equation 35 need no longer be obeyed strictly, i.e. the residence time of marked material is no longer assumed to be identical with the average volumetric residence time. This is a simplification of the same order as replacing the real mass transport boundary layer with a Nernst diffusion layer, which is an *equivalent* boundary layer, and, similarly, it allows the systematic evaluation of experimental data as will be shown in Part II. It has been shown that, in general, very many electrochemical reactors can be described by two-phase models [12, 13].

7. Radial inflow

If the direction of the flow is reversed so that it moves towards the centre (sink flow) then the analagous equation to Equation 2 is

$$\frac{\partial c}{\partial t} = \bar{D}\frac{\partial^2 c}{\partial r^2} + \frac{\bar{D}}{r}\frac{\partial c}{\partial r} + \frac{Q}{2\pi r}\frac{\partial c}{\partial r} \quad (37)$$

which transforms to

$$\frac{d^2\bar{c}}{dr^2} + \frac{(1+2\nu)}{r}\frac{d\bar{c}}{dr} - \frac{s}{\bar{D}}\bar{c} = 0 \quad (38)$$

where $\nu = Q/4\pi\bar{D}$.
Using $\lambda = r(s/\bar{D})^{1/2}$ as before, but now assuming a solution of the form

$$\bar{c} = \lambda^{-\nu}\omega \quad (39)$$

one obtains

$$\frac{d^2\omega}{d\lambda^2} + \frac{1}{\lambda}\frac{d\omega}{d\lambda} - \left(1 + \frac{\nu^2}{\lambda^2}\right)\omega = 0 \quad (40)$$

as before (Equation 11). The appropriate solution is now I_ν, which tends to a finite limit as $r \to 0$, rather than K_ν which tends to infinity, so the response to a step function injected at $r = r_o$ is given by

$$\bar{c} = \frac{c^o}{s}\left(\frac{r_o}{r}\right)^\nu \frac{I_\nu[(s/\bar{D})^{1/2}r]}{I_\nu[(s/\bar{D})^{1/2}r_i]} \quad (41)$$

Proceeding to the moments as before one obtains

$$\bar{D} = \frac{(r_o^2 - r^2)}{4M_1\left\{\frac{(r_o^2 + r^2)}{(r_o^2 - r^2)}\frac{M_1^2}{(M_2 - M_1^2)} - 1\right\}} \quad (42)$$

again enabling $\bar{D}$ to be estimated from the moments.

8. Experimental results

Fig. 4 shows the response curves for geometrically identical capillary gap (disc-stack) and pump cells obtained under the same conditions of volumetric flow rate. Clearly the shapes of the responses are different in the two cases, those for the pump cell, where the coupling of tangential swirl has made the axial velocity profile more uniform [8], being noticeably more plug-like and quite similar in form to the theoretical shapes of Figs. 2 and 3. The analyses of these and other responses will be discussed more fully in Part II, but it is clear that the plug-flow model provides a basis on which to proceed provided that plug flow is not considered to fill the entire inter-electrode gap.

9. Summary and conclusions

A simple dispersive plug-flow model has been developed which permits the estimation of an effective dispersion coefficient through the first and second moments of the response curve for a pulse of electrogenerated species at the wall. The ratio of the first moment of the response curve to the mean plug-flow residence time gives an estimate of the segregation of the fluid in such systems. An improved model of fast and slow phases with mass exchange between them, arising out of this first order model, is receiving attention.

References

[1] F. Beck and H. Guthke, *Chimie Ingnr. Techn.* 41 (1969) 943.

[2] M. Fleischmann, R. E. W. Jansson, G. A. Ashworth and P. J. Ayre, British Prov. patent no. 18 305/74.
[3] R. E. W. Jansson and R. J. Marshall, *Chem. Engr.* **315** (1976) 769.
[4] M. Fleischmann, R. E. W. Jansson and R. J. Marshall, British Prov. patent no. 04 939/76.
[5] M. Fleischmann and R. E. W. Jansson, Keynote lecture at the *Symposium on Electro-organic Synthesis, 84th National Meeting* AIChE, Atlanta, Georgia (1978).
[6] N. R. Tomov, PhD thesis, Southampton University (1978).
[7] R. Dworak and H. Wendt, *Ber. Bunsengesellschaft Phys. Chim.* **80** (1976) 78.
[8] J. Ghoroghchian, PhD thesis, Southampton University (1978).
[9] I. H. Justinijanovic, PhD thesis, Southampton University (1975).
[10] 'Higher Transcendental Functions', Vol. 2, Bateman Manuscript Project, McGraw-Hill (1953).
[11] O. Levenspiel, 'Chemical Reaction Engineering', John Wiley Inc., New York (1962).
[12] Z. Ibrisagic, PhD thesis, Southampton University (1977).
[13] M. Fleischmann, R. E. W. Jansson and R. J. Marshall, to be published.
[14] M. Abramowitz and I. A. Stegun, 'Handbook of Mathematical Functions', Dover Publications (1965) pp. 358, 374.